ICOLD Symposium on Sustainable Development of Dams and River Basins, 24th - 27th February, 2021, New Delhi

ASSESSMENT OF CONCRETE PROPERTIES OF BHAKRA DAM IN INDIA

BRIJESH SINGH, V V ARORA, P N OJHA, B N MOHAPATRA AND VIKAS PATEL
National Council for Cement & Building Materials, Ballabgarh, Haryana, India

PRAMOD NARAYAN AND BIKRAM K PATRA
Dam Safety Rehabilitation Directorate, Central Water Commission, Delhi, India

ABSTRACT

The concrete gravity dam under the present study is more than 50 years old and to execute an accurate and reliable analysis, complete chemical and physical analysis of concrete properties are required. Therefore, keeping in view the importance of the structure, Central Water Commission desired data/information on concrete and rock properties for conducting advanced Finite Element Analysis (FEA) of Bhakra Dam to study unusual deflection of the dam. This paper presents a case study of the Bhakra dam under the ongoing Dam Rehabilitation and Improvement Project (DRIP) in India. The complete investigations of mechanical properties include field assessment, thermal properties, and expansion issues. The concrete core samples from the dam were used to determine mechanical properties, chemical properties, petrographic studies, surface morphology study of concrete samples by the Scanning Electron Microscopic (SEM) method including detection of ettringite presence and fracture pattern, X-Ray Diffraction analysis and Alkali Aggregate Reactivity. Testing on rock samples from left and right bank on the downstream side of Dam for determining volumetric weight, Modulus of Elasticity Poisson's Ratio, Uni-axial Compressive Strength, Ultrasonic Pulse Velocity (UPV) (P-wave only) and permeability co-efficient of the rock mass (laboratory test only) are also presented in the paper. Based on the study, it is seen that the overall quality of concrete is sound and the experimental test results of compressive strength, modulus of elasticity, Poisson's ratio and split tensile strength are in a similar range to the designed values for these parameters. The test results of the resistivity test and humidity meter indicate that moisture content in the upstream side is higher than the downstream side. The impact of aggregate and other concrete constituents on the deterioration of concrete which can have a significant impact on the durability and safety of the dam are discussed. The chloride, sulphate, pH and all other chemical parameters are within the permissible limit given in IS: 456-2000 for both concrete and water.

1. INTRODUCTION

Concrete gravity dams are large and complicated structures that are expected to withstand various usual loads and seismic effects without an unacceptable level of damages. Due to aging, the dams are subjected to severe environmental conditions that affect the strength and ultimately the seismic performance of the concrete dams. Therefore, in order to execute an accurate and reliable analysis for concrete dam, it is necessary to estimate the properties of concrete in dam appropriately. Especially in the concrete dams, the stresses caused by temperature changes can be larger than those from the reservoir loading. The effects of temperature change depend on the thermal properties of the concrete (PK Mehta 1986, Neville 1986 & MK Hoowlader 2012). The two important chemical reactions which have a capability to cause swelling in concrete dams are Alkali Aggregate Reaction (AAR) and Ettringite Formation (EF) (LS Dent et.al. 1981, D Heinz et.al. 1997, HFW Taylor et.al. 2001, BG Wigum et.al. 2006, A Sellier 2009 & RP Martin 2010). They lead to an expansion of the material and induce generally cracking and degradation of the mechanical properties. This implies problems in terms of serviceability, structural integrity (S Malla et.al. 1996, JF Seignol et.al. 2009 & P Rivard et.al. 2010) and durability since cracking favors the ingress of external species prone to initiate other degradations. To deal with the affected structures, it is thus necessary to precisely understand the chemo-mechanical effects of each reaction. In the present investigation, assessment of concrete properties for Bhakra Dam in India having more than 50 years age is presented. The Bhakra Dam, located near village Bhakra in district Bilaspur of Himachal Pradesh, is a 225.55m (740 ft.) high straight gravity concrete dam, built across river Sutlej in a deep and narrow gorge of the Lower Siwalik Hills. The length and width of the dam at the top is 518.16 m (1700 ft.) and 9.14 m (30 ft.) , respectively, with the width of dam at base being kept as 190.5 m (625 ft.) and the width including apron and heel claystone plug as 402.33 m (1320 ft.). In the concrete gravity dam no major distress was observed and health monitoring investigation was undertaken. The interpretation of field and laboratory studies including microstructure studies of concrete in the dam are evaluated in order to have accurate and reliable Finite Element Modelling dam for determining reason behind unusual deflection of dam. A separate paper, enumerating on the findings of the 3D numerical model Bhakra is also prepared for ICOLD 2020.

2. FIELD STUDIES ON CONCRETE GRAVITY DAM

The Non-Destructive tests were conducted in the galleries (both inside and outside) and the accessible portions of downstream and upstream of the dam. The tests mainly include Ultrasonic Pulse Velocity (UPV) test, Half Cell Potential Test, In-situ moisture content using humidity meter, Resistivity test & Air permeability test. The UPV test measurements done by the surface probing method as per IS: 13311 Part-I-1992 with pulse velocity varied between 3.56 km/sec to 4.03 km/sec. When these values are compared with the velocity criteria of IS: 13311 (Part 1)–1992, the overall quality of concrete is assessed to be “Good” in general. The Half-cell potential measurements were taken at nine different locations and when these results were compared with the corrosion criteria as per ASTM C-876, it is seen that there is no corrosion of reinforcing bars i.e. 90 % chance of no corrosion. The chemical analysis of concrete core samples was carried out and from the results, it is seen that the pH values are on the higher side indicating no loss of passive layer around the reinforcement which protects the steel from distress. The moisture content in-situ readings were taken at eight different locations along the downstream side, upstream side and four galleries at different elevations. The moisture content varied from 4.64% to 5.20%. The moisture content on the upstream side varied from 4.95 to 5.20 percent and on the downstream side, it was around 4.64 %. The test results indicate that moisture content in the upstream side is marginally higher than the downstream side.

The coefficient of Air Permeability (kT X10-16) for U/S right bank, U/S left bank, Gallery at Elevation 1073’ upstream and Gallery at Elevation 1608’ downstream varied from 0.016 to 0.046 which indicated that quality of near-surface concrete falls in Good category. The coefficient of Air Permeability (kT X10-16) for D/S right bank at Elevation, D/S left bank at Elevation, Gallery at Elevation 1268’ upstream and Gallery at Elevation 1548’ downstream varied from 0.269 to 0.590 which indicated that quality of near-surface concrete falls in Normal category. The values of electrical resistivity range from 77.00 kΩcm to 95.37 kΩcm. The test results indicate that moisture content in the upstream side is marginally higher than the downstream side and the same is confirmed by humidity meter test results. Ambient temperature, CO2 level, and humidity were measured randomly at the downstream side, upstream side and four galleries at different Elevations. The ambient temperature varied from 23.0˚C to 28˚C and CO2 level varied from 274 ppm to 497 ppm. Humidity level varied from 27.80 % to 72.00 %. The variation between the ambient temperature on the Downstream Side and Upstream Side concerning the gallery at four different elevations was about 2 to 3˚C. This data is reported based on the field investigation carried out by NCB for a particular period and the data may vary seasonally and CO_2 level may vary over the period of the year. No Carbonation was observed in all the concrete samples when concrete is exposed and sprayed with 1% phenolphthalein solution in ethanol at all the locations.

3. SAMPLE COLLECTION AND LABORATORY TESTS

The concrete core samples were extracted (Figure -1) from all the accessible portions of the dam covering the entire structure. Total numbers of 100 concrete core samples of 150 mm and 100 mm diameter were tested. Visual observation of all the accessible portions of four Galleries including the upstream and downstream portion of the dam was carried out at the site and the concrete core samples extracted from different locations were also observed for any abnormal reaction in concrete. During the site inspection, based on data recorded by dam authority, it was informed at the site that the upstream side of the dam face is most exposed to solar radiation during the summer period. No signs of distress in concrete was apparently visible during the site inspection. The visual inspections of concrete cores as extracted indicated dense and well-compacted concrete.

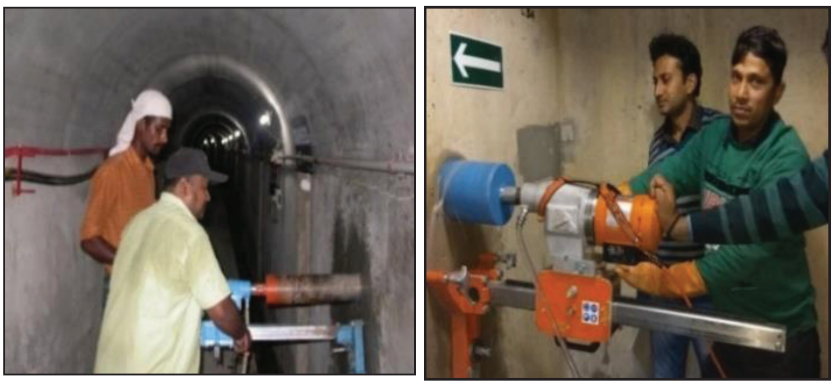

Figure 1 : Concrete Core Extraction in Gallery of Dam

The equivalent cube compressive strength was determined on hardened concrete core samples of 150 mm and 100 mm diameter extracted from the dam as per IS:516. The concrete core specimens were tested in a strain-controlled compression testing machine of 3000 KN capacity (Figure 2) at room temperature of 27±2oC and relative humidity 65% or more. Two extensometers in the middle half of the height were used to get strain and two strains were averaged. Both ends of concrete cylinders were finished parallel by grinding.

Figure 2 : Test setup for uni-axial compression testing of concrete in Strain Controlled Machine (3000 KN)

The comparison of designed concrete strength for type A (3 ft. thick concrete on surroundings of galleries), B (Mass Concrete) and C (6 ft. thick concrete on upstream face) concrete used in the dam and experimentally obtained equivalent cube compressive strength under present investigation is given below in Table-1. For Concrete Type A: Poisson's Ratio: 0.21, Modulus of Elasticity: 25265 N/mm^2 & Split Tensile Strength: 2.04 N/mm^2. For Concrete Type B: Poisson's Ratio: 0.20, Modulus of Elasticity: 25955 N/mm^2 & Split Tensile Strength: 3.39 N/mm^2. For Concrete Type C: Poisson's Ratio: 0.20, Modulus of Elasticity: 27691 N/mm^2 & Split Tensile Strength: 2.52 N/mm2. The coefficient of thermal expansion values for Type-A concrete vary from 9.09 X 10-6 to 14.71 X 10-6, for Type-B concrete vary from 9.91 X 10-6 to 14.05 X 10-6 and for Type-C concrete vary from 9.21 X 10-6 to 13.92 X 10-6 respectively. The average coefficient of Permeability values for Type-A, Type-B, and Type-Concrete are 3.07 X 10-11, 3.10 X 10-11 and 4.54 X 10-11 respectively.

Table 1 : Test Results Concrete Compressive Strength

Sl. No.	Concrete Type	Designed Concrete Strength (N/mm^2)	Equivalent Cube Compressive Strength (N/mm^2)	
			Range	Average
1.	A (3 ft. thick concrete on face of Galleries)	17.25	16.29 to 24.72	22.04
2.	B (Mass Concrete)	15.85	18.32 to 35.98	27.44
3.	C (6 ft. thick concrete on Upstream face)	20.70	23.62 to 29.89	26.31

4. CHEMICAL ANALYSIS AND MINERALOGICAL STUDIES OF CONCRETE

The data on cement (content, SO3 and Na2O equivalent) was not available. However, the SO3 content calculated from the chemical analysis of concrete core samples in the case of gravity dam varied from 0.12 to 0.34 % per m^3 of concrete and Na2O equivalent (water-soluble acid method) in the concrete of gravity dam varied from 0.86 to 1.10 per m^3 of concrete. The chloride, sulfate, pH and all other chemical parameters are within the permissible limit given in IS: 456-2000 for both concrete and water. No adverse chemical presence in concrete and water samples, in general, is seen. From literature, it is seen that the total mass of alkali in the concrete mix shall not exceed 3 kg per m^3 of concrete and in the present investigation also the values are well below the limit 3 kg per m^3. The detailed mineralogical investigation such as petrographic studies of aggregate and concrete, presence of any reactive or abnormal products and Alkali Aggregate Reactivity (AAR) attack or sulfate attack is crucial from detecting the cause of distress if any in the aged concrete. The petrographic studies of rock types present in the concrete cores extracted from the dam were carried out and the details of petrography analysis are discussed below. The petrographic analysis of coarse aggregate indicates a major aggregate type as sedimentary (quartzite & sandstone). The modal compositions of the rock types are given below in Table 3:

Table 3 : Modal Composition of Coarse Aggregates (Results in %)

Rock Type	MINERALS											
	Quartz	**Orthoclase-Feldspar**	**Plagioclase-Feldspar**	**Biotite**	**Muscovite**	**Microcline-Feldspar**	**Calcite**	**Hornblende**	**Tourmaline**	**Garnet**	**Pyrite**	**Iron Oxide**
Quartzite	91	-	-	2	1	-	-	-	-	-	4	2
Feldspathic Sandstone	65	12	7	1	1	10	-	-	-	-	3	1
Sandstone	88	4	-	4	1	-	-	-	-	-	2	1
Calcareous Sandstone	87	2	3	1	1	-	4	-	-	-	1	1
Micaceous Sandstone	82	4	-	11	2	-	-	-	-	-	-	1
Granite	37	16	14	13	3	8	-	3	2	1	2	2

The Petrography analysis of concrete samples indicates there is no Alkali-Silica Reaction in the concrete. From the petrography study, five different major rock types and one minor rock type (Granite) were found. For estimating the percentages of different types of coarse aggregates, samples were taken out from concrete cores representing different locations. The total weight of the coarse aggregates in overall concrete separated based on the petrographic examination was approximately 90 Kg. In the petrographic analysis, various rock types namely Quartzite, Feldspathic sandstone, Calcareous sandstone, Micaceous sandstone, and Granite were observed. The percent distribution of these different rocks types in the total weight of the coarse aggregate was calculated and the percentage of the rocks are as follows: Quartzite-25.33%, Feldspathic sandstone–23.32%, Sand stone-23.13%, Calcareous sandstone- 12.48%, Micaceous sand stone-11.13%, and granite rocks- 4.59%. A similar exercise was repeated for calculating the percent distribution of various rock types in the coarse aggregates of rich concrete and mass concrete. The percent distribution of various rocks types present in rich concrete A and C were analyzed. In the petrographic analysis, various rock types namely Quartzite, Feldspathic sandstone, Calcareous sandstone, and Granite were observed. The percent distribution of these different rocks types in the total weight of the coarse aggregate was calculated and the percentage of the rocks is as follows: Quartzite-30.99 %, Feldspathic sandstone–13.20%, Calcareous sandstone- 30.60% and Granite- 25.10%. The distribution of aggregates types in mass concrete (B) was analyzed and various rock types namely Quartzite, Feldspathic sandstone, Sandstone, Calcareous sandstone, Micaceous sandstone, and Granite were observed. The percent distribution of different rock types in the total weight of the coarse aggregate was calculated and the percentage of the rocks are as follows: Quartzite-30.20%, Feldspathic sandstone–13.50%, Sand stone-28.90%, Calcareous sandstone- 14.40%, Micaceous sandstone- 8.60%, and Granite- 4.10%. However, the overall percentage of the rocks in this category may also vary when the total mass of the rocks used in the mass concrete of the Dam is considered. The petrographic analysis results indicate the presence of Pyrite (FeS_2) in a variable percentage (1-4%).

The concrete core samples were also tested for Scanning Electron Microscope (SEM) Study. The concrete core samples were divided into three categories namely Upstream, gallery, and Downstream. The numerous open-air voids of various shapes and sizes with smooth margins are uniformly distributed in the concrete. The growth of perfect ettringite crystal mostly in radiating needle form is observed. The ettringite crystals are mainly developed in small size open-air voids. Few voids are filled with radiating needle-shaped ettringite microcrystals (Figure 3). The growth of both convergent and divergent type radiating microcrystals of ettringite is noticed within the voids. In a few instances, the microcrystalline ettringite grains (Figure-4) are spread outside the voids. The formation of more ettringite crystals was in progress within the voids. Twinned crystals of ettringite are also observed in a few clusters. The ettringite crystals are tightly packed. This ettringite may further grow into bigger size crystals. No Alkali-Silica-Reaction rims are observed between coarse aggregates and mortar in these concrete cores.

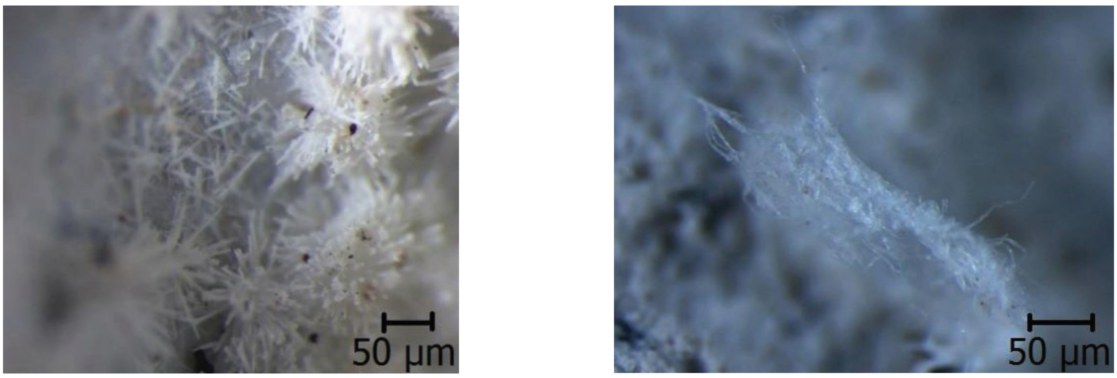

Figure 3 : Growth of complex structured ettringite crystals in cluster form in the Air Void

The sulfate in the form of pyrite was found in the aggregates from petrographic, SEM and XRD studies and this is the reason for crystalline ettringite formation. Ettringite percentage in open-air voids is maximum in upstream samples (3 to 4% of open-air voids) and minimum in the gallery and downstream samples (1 to 2% of open-air voids). Percentage of crystalline ettringite present in open-air voids is about 2% of open-air voids in mass concrete. The percentage of crystalline ettringite in mass concrete of upstream, gallery and downstream samples varies from 0.01 to 0.03 %. The ettringite formation of such a small magnitude is not likely to cause any expansion and it is also reported in the past that the ettringite, found in this benign state as large needle-like crystals, should not be interpreted as causing the expansion of deteriorating concrete (PCA R&D 2002). However, it was recommended to conduct periodic inspections on selected samples after five years to understand the growth rate of ettringite formation in the future.

The X-Ray Diffraction (XRD) analysis of the samples collected from the upstream, galleries and downstream concrete core samples show the minor peaks of Ettringite, Portlandite, Akermanite, and Larnite. The intensity of Ettringite peaks in all these samples is low, which indicates that these concrete samples have a low concentration of ettringite crystals. A minor percentage of unconsumed Larnite was still present in the concrete of higher elevation, which may hydrate in the later stage. Portlandite and Akermanite peaks indicate the hydration products of the cement used. It is seen that there is no significant unhydrated part left in the samples and no extraordinary phases are identified. Minor ettringite formation is also detected. In XRD results, no symptom of Alkali-Silica-Reaction is observed.

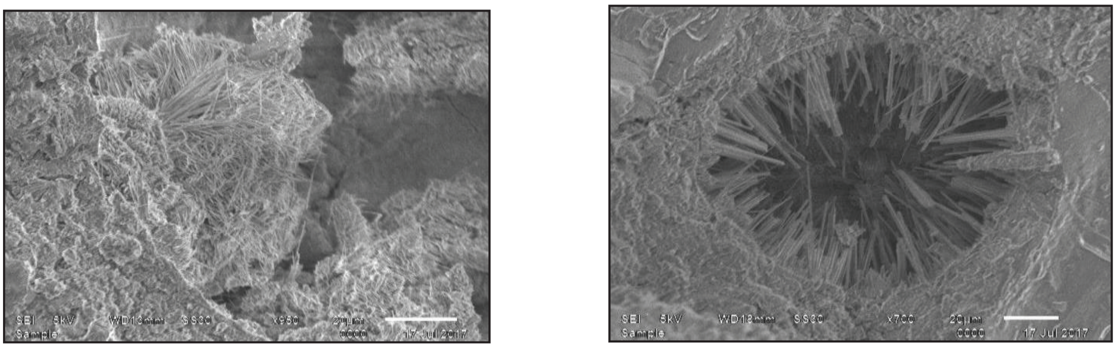

Figure 4 : Scanning Electron Microscope images of ettringite in air Void of concrete sample

The detection of Alkali-Silica Reaction swelling in concrete by staining method (color test) was done based on the method proposed by GD Guthrie et.al. 1997. The study included the sequential application of solutions of each of the two water-soluble compounds. Concentrated solutions of sodium cobaltinitrite and rhodamine B in water are prepared. The concrete surface to be examined was treated by pre-rinsing with water and subsequently applying each solution to the surface. After 30-60 seconds, the concrete was rinsed thoroughly with water. The treated surface will show yellow and pink regions where ASR gel is present, yellow regions indicate the presence of K-rich, Na-K- Ca-Si gels. While pink regions indicate alkali-poor gels. The final rinse step was required, since the yellow sodium cobaltinitrite solution will coat the entire concrete surface as will the pink rhodamine B solution, thereby obscuring the stained gel regions. Best results were obtained when the sample is treated first with the sodium cobaltinitrite solution; however, the application of the rhodamine B solution first gave adequate results. The slice of concrete core samples was rinsed with water and rinsed surfaces were searched for regions of yellow staining and regions of pink staining whereby K-rich i.e. Na-K-Ca-Si gels generated from ASR were identified by yellow staining and alkali poor, Ca-Si generated from ASR were identified by pink staining. Four concrete core samples were selected keeping in view the total representation of upstream and downstream for the presence of ASR using the color method. The treated samples were searched for regions of yellow staining (K-rich i.e. Na-K-Ca-Si gels generated from ASR) or regions of pink staining (alkali poor i.e. Ca-Si generated from ASR). The color test results indicate that the concrete core samples are free from Alkali-Silica Reaction (Figure-5). In a few instances, very minor reaction rims are developed on the margins of large size open-air voids. If the total area of the concrete is considered the area shows reaction rims are negligible. However, a detailed analysis of the color test was done both in the optical microscope and scanning electron microscope.

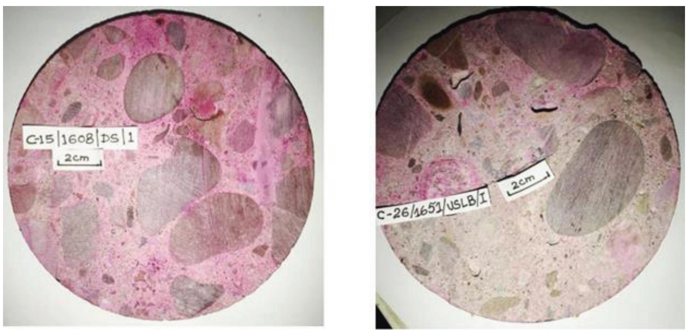

Figure 5 : Colour Test on Downstream and Upstream Gallery Samples

The 14 days results of accelerated Mortar Bar Test as per ASTM C-1260 (2014) for coarse aggregate taken from concrete cores and measured using mortar bars of 25 mm x 25 mm x 285 mm indicated that the net expansion in the coarse aggregate sample is 0.08 %. The test results of accelerated Mortar Bar Test conducted on the concrete core in similar lines to ASTM C-1260 (2014) for determining residual expansion indicated the net expansion 0.04 %. As the residual net expansion of concrete samples is less than 0.1 % the aggregates were not under potentially reactive category and there is no potential ASR in concrete. The concrete core specimens from both wet and dry portions of the dam were selected for residual expansion testing in a similar line to the procedure in ASTM C 1293 (2018) to determine the susceptibility of concrete to the alkali-silica reaction. The concrete core was tested with a deviation that temperature was changed from 38 ˚C to 60 ˚C. The change in temperature was done from 38 ˚C to 60 ˚C because it was seen in the past studies done by NCB that the slow reactive aggregate gives expansion at 60o C. The higher temperature has been also recommended in IS: 2386 Part VII and IS: 383-2016 also. The average residual expansion of concrete cores in the case of a gravity dam varied from 0.0231 to 0.0271 % (Figure-6). This average residual expansion after more than 50 years of age is not significant keeping in view that the limit is 0.04 % at the age of one year and thus, it indicates no potential of Alkali-Silica Reaction.

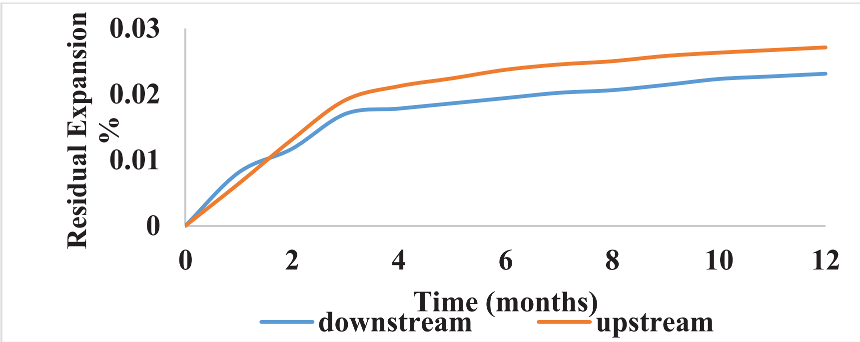

Figure 6 : Residual expansion of concrete cores by ASTM C1293 (2018) method

The in-situ properties of concrete obtained from the investigation was used in the advanced FEM modeling of dam wherein basic objective was to get reliable model output about the realistic deformations, stresses, inclination etc. to study unusual deflection of dam conducted under ongoing Dam Rehabilitation and Improvement Project (DRIP).

5. STUDY ON MECHANICAL PROPERTIES OF ROCK SAMPLES

About 10 rock samples of 150 mm and 100 mm diameter were extracted from the rock near the left bank and Right bank on the downstream side. The test results of rock samples are given in Table-2. The equivalent cube compressive strength of rock samples of 150 mm diameter varies from 54.75 N/mm2 to 68.80 N/mm2 with an average compressive strength of 64.60 N/mm2. Poisson's Ratio of rock samples varies from 0.171 and 0.209 with an average of 0.186. The Modulus of Elasticity of rock samples varies from 14135 N/mm2 to 15794 N/mm2 with an average of 14944 N/mm2. The dry density and wet density of the rock cores vary from 2589.30 Kg/m3 to 2643.68 Kg/m3 and 2614.66 Kg/m3 to 2669.51 Kg/m3 respectively. Petrography study of rock sample indicated that rock is a fine to a medium-grained textured, poorly foliated, partially weathered random sample. The Ultrasonic Pulse Velocity values from rock cores vary from 2.93 km/sec to 3.41 km/sec. One of the reasons for lower pulse velocity and modulus of elasticity as indicated from petrographic studies is that rock samples under investigation are fine to medium-grained textured, poorly foliated and partially weathered.

The Co-efficient of Permeability for rock samples was determined using a relationship developed between Permeability and Porosity of the sedimentary rocks by Na Zhang et al. (Pore structure characteristics and permeability of deep sedimentary rocks determined by Mercury Intrusion Porosimetry). The porosity of rocks extracted from the left and right bank on the downstream side portion of Dam were obtained using Mercury Intrusion Porosimetry. The permeability coefficient of rock mass was determined using the Mercury Intrusion Porosimeter apparatus (PASCAL 140 and PASCAL 440) having the capability of determining pore size and volume in the range of 1.8 and 7500 nm of radius, through mercury intrusion at high pressure. The porosity values (%) obtained for left and right bank rock samples were 6.397 and 6.543 respectively. The following relationship developed by Na Zhang et al were used for calculating permeability.

$$K = 2*10^{-6} e^{0.3241\Phi}$$

Where K represents Permeability in Milli Darcy (MD) and Φ (%) is Porosity

The Co-efficient of Permeability values (Milli Darcy) obtained for left and right bank rock samples were 1.59 x 10^{-5} and 1.66 x 10^{-5} respectively.

Table 4 : Test Results of Rock samples

Sl. No.	Modulus of Elasticity (MPa)	Poisson's Ratio	Compressive Strength (MPa)	Wet Density (kg/m³)	Dry Density (kg/m³)	UPV (P wave Velocity) km/sec
1	-	-	67.12	2643.72	2622.61	2.88
2	14135	0.187	65.17	2614.66	2589.30	3.09
3	15794	0.177	61.12	2669.51	2643.68	3.08
4	14869	0.209	69.83	2664.57	2633.57	3.29
5	-	-	54.74	2620.68	2595.13	2.93
6	14976	0.171	68.80	2659.26	2642.46	3.41

6. CONCLUSIONS

The field studies indicate that there is no carbonation and corrosion activity taking place inside the concrete structure of the dam. The overall quality of concrete is sound and the experimental test results of compressive strength, modulus of elasticity, Poisson's ratio and split tensile strength are in a similar range to the designed values for these parameters considered in the design. The test results of the resistivity test and humidity meter indicate that moisture content in the upstream side is higher than the downstream side.

The petrographic analysis of coarse aggregate indicates aggregate to be non-reactive for alkali aggregate reaction and major aggregate type as sedimentary (quartzite & sandstone). The sulfate in the form of pyrite was found in the aggregates from petrographic, SEM and XRD studies and this is the reason for crystalline ettringite formation. Ettringite percentage in open-air voids is maximum in upstream (3-4% of open-air voids) and minimum in the gallery and downstream (1-2% of open-air voids). Percentage of crystalline ettringite present in open-air voids is about 2% of open-air voids in mass concrete. The percentage of crystalline ettringite in mass concrete of upstream, gallery and downstream samples varies from 0.01 to 0.03 %. The ettringite formation of such a small magnitude in large voids does not cause any expansion. The results of Accelerated Mortar Bar Test conducted on concrete cores in similar lines to ASTM C-1260 (2014) for determining residual expansion indicated the net expansion 0.04 %. The average residual expansion of cores similar to the procedure of ASTM C-1293 (2018) varied from 0.0231 to 0.0271 %. This average residual expansion after more than 50 years is not significant keeping in view that the limit is 0.04 % at the age of one year and thus, it indicates no Alkali-Silica Reaction. However, it was recommended to conduct periodic inspections on selected concrete after every five years interval to understand the growth rate of ettringite formation in the future. The results of petrography studies, SEM studies, color test and accelerated test on cores indicates there is No Alkali-Silica Reaction in concrete.

The Ultrasonic Pulse Velocity (P wave only) values for rock cores extracted from the left bank and Right bank on downstream side varies from 2.93 km/sec to 3.41 km/sec. The overall average values of Compressive Strength, Poisson's Ratio, Modulus of Elasticity and Coefficient of permeability are 64.60 N/mm2, 0.186, 14944 N/mm2, 1.59 x 10-5 (for the left bank) and 1.66 x 10-5 (for the right bank) respectively. One of the reasons for lower pulse velocity and modulus of elasticity as indicated from petrographic studies is that rock samples under investigation are fine to medium-grained textured, poorly foliated and partially weathered.

The in-situ properties of concrete obtained from the study have been used in the advanced FEM modeling wherein basic objective remains to get reliable model output about the realistic deformations, stresses, inclination etc. to study unusual deflection of the dam.

ACKNOWLEDGEMENTS

The authors would like to acknowledge the NCB laboratory technical officers and technical assistants, Central Project Management Unit DRIP, Central Water Commission-India, BBMB as well as World Bank for their assistance in carrying out this sponsored project.

REFERENCES

ASTM C1260 (2014): *Standard Test Method for Potential Alkali Reactivity of Aggregates (Mortar-Bar Method)*

ASTM C1293 (2018): *Standard Test Method for Determination of Length Change of Concrete Due to Alkali-Silica Reaction*

Dent Glasser LS & Kataoka N (1981): *The chemistry of alkali-aggregate reactions*. Advances in cement Research (18): 47-63

Heinz D & Ludwing U (1987): *Mechanism of secondary ettringite formation in mortars subjected to heat treatment*. ACI SP 100, Detroit, USA: 2059-2071

IS 2386 Part-VII (1963): *Indian Standard methods of test for aggregate for concrete, Part-VII Alkali Aggregate Reactivity*

IS 2386 Part-VIII (1963): *Indian Standard methods of test for aggregate for concrete, Part-VIII Petrographic examination*

IS 456 (2000): *Indian Standard for plain and reinforced concrete -code of practice*

IS 383 (2016): *Indian Standard for coarse and fine aggregate for concrete-specification*

Martin RP (2010): *Experimental analysis of the mechanical effects of delayed ettringite formation on concrete structures*. Ph D thesis, University of Paris, PP-577

Mehta PK (1986): *Concrete Microstructure, Properties and Materials*. Prentice-Hall International Series in Civil Engineering and Engineering Mechanics

Milon K Hoowlader (2012): *Effects of aggregate types on thermal properties of concrete*. Deptt. of Civil Engg. Bangladesh, ARPN Journal of Engineering and Applied Sciences, Vol.7, 900-907

Neville AM (1996): *Properties of Concrete*. 4th Edition, ELBS, Addison Wesley Longman Limited, Harlow, England, ISBN

PCA (2002): *Ettringite formation and the performance of concrete,* Concrete Information, 5420 Old Orchard Road Skokie, Illinois, USA, PCA R&D Serial No. 2166, IS417.01

Rivard P, Bllivy G, Gravel C & Saint-Pierre F (2010): *Monitoring of a hydraulic structure affected by ASR: A case study.* Cement and Concrete Research (40): 676-680

S Malla & M Wieland (1996): *Analysis of Arch Gravity Dam with a horizontal crack*. Electrowatt Engineering Limited, Bellerivestrasse, Zurich, Switzerland, Computers and Structures, 267-278

Seignol JF, Bagdadi N & Toutlemonde F (2009): *A macroscopic chemo-mechanical model aimed at re-assessment of delayed ettringite formation affected concrete structures*. May 24-27, Korea: 422-440

Sellier A, Bourdarot E, Multon S, Cyr M & Grimal E (2009): *Combination of Structural monitoring and laboratory testing for assessment of alkali-aggregate reaction swelling: application to gate structure dam*. ACI Materials Journal (106-3): 281-29

Taylor HFW, Famy C & Scrvener KL (2001): *Delayed Ettringite Formation*. Cement and Concrete Reseach (31): 683-693

Wigum BJ, Pedersen LT, Grelk B & Lindgard J (2006): *State-of-the-art report: Key parameters influencing the alkali aggregate reaction*. Report 2.1, SINTEF: PP: 56

Guthrie GD & Carey JW (1997): *Detection of alkali-silica reaction swelling in concrete by staining*. Cement and Concrete Research, Vol. 27, No. 9, pp. 1407–1417